MODELLING OF THE EFFECTIVENESS OF Al-Ti-B REFINERS IN COMMERCIAL PURITY ALUMINIUM

A.M. Bunn, P. V. Evans[*], D. J. Bristow[†] and A.L. Greer

University of Cambridge, Department of Materials Science & Metallurgy, Pembroke St., Cambridge CB2 3QZ, UK

[*]Alcan International Ltd, Banbury Laboratory, Southam Rd, Banbury, Oxon OX16 7SP, UK

[†]London & Scandinavian Metallurgical Co. Ltd., Fullerton Rd, Rotherham, S60 IDL, UK

Abstract

Al-5Ti-1B (wt.%) alloys are effective grain refiners for DC-cast aluminium although as few as 1% of the TiB_2 particles added to the melt nucleate grains. The aim of this work is to develop quantitative modelling for prediction of grain sizes in commercial purity aluminium. In this way the low efficiency of refiners can be understood, ultimately to clarify the design rules for a more effective refiner. The modelling focuses on the role of particle size distribution. This is in conjunction with measurements (by scanning electron microscopy and image analysis) of the particle size distributions in commercial Al-5Ti-1B refiners known to have differing performances. The undercooling required for heterogeneous nucleation of α-Al on the surface of potent TiB_2 particles is extremely low. Accordingly, the modelling is based on the assumption that the critical step for a particle to behave as an active growth centre is that required to initiate free growth from the particle surface, rather than the initial heterogeneous nucleation event. It is considered that further initiation of free growth of crystals is stopped by the onset of recalescence in the melt during solidification. Only those particles which are active growth centres at the point of recalescence will contribute towards the final grain size. Negligible interference between particles and spherical growth up to the point of recalescence are assumed; these assumptions are rigorously tested. The model tests the effect of varying the particle size distribution by using measured distributions from 'good' and 'poor' refiners. The variation of grain size with addition rate of refiner is examined. The model predicts an effective saturation, beyond which further addition has little effect. In general, good agreement is found between the grain-size predictions and conventional grain-refining tests.

Introduction

Al-Ti-B refiners are used to promote fine grain structures in castings, producing a typical grain diameter of ~200 μm. Heterogeneous nucleation of α-Al occurs on the (0001) basal faces of hexagonal platelet TiB_2 particles, coated with a thin layer of Al_3Ti [1,2]. At most, ~1% of the particles present in the refiner are active in nucleating grains [3]. Some of the particles will not nucleate grains because of inhomogeneous heat and fluid flow conditions in the melt, and some inherent differences in potency [4]. However it is considered in this work that the low efficiency of refiners is largely due to recalescence of the melt, as proposed by Maxwell and Hellawell [5]. However, the initiation of free growth of α-Al from added inoculant particles is considered to be the rate-limiting step, rather than heterogeneous nucleation on the particles. Also, the analysis in [5] is extended by considering the effects of particle size *distributions*, and the assumptions of spherical growth and negligible re-melting of crystals are re-examined.

Maxwell and Hellawell [5] modelled the heterogeneous nucleation of α-Al in an isothermal melt containing inoculants. They showed that the ratio of number of grains to number of nucleating particles is unity for very low addition levels of inoculant but becomes very small at higher addition levels, the grain density tending to saturate at a level dependent on a number of factors. The saturation and low efficiency are consequences of latent heat release causing recalescence of the melt and precluding further nucleation events. Maxwell and Hellawell [5] showed that inoculant efficiency is significantly greater for: more potent nucleating substrates (lower contact angle), greater cooling rate, and greater growth restriction by solute (investigated for three alloy systems). They also investigated the effect of inoculant particle size (the heterogeneous nucleation rate on a particle being taken to be proportional to its surface area), but found only a small effect. Hodaj and Durand [6] extended this model to multicomponent alloys assuming that the total solutal undercooling is the sum of the contributions of each solute element.

Condition for Free Growth

The classical model for heterogeneous nucleation involves a spherical cap, for which the work of nucleation is reduced compared to the spherical homogeneous nucleus. The lower the contact angle for the cap on the inoculant surface, the easier the nucleation. However in the case of Al-Ti-B refiners (and other very potent inoculants) nucleation undercoolings as low as 0.01 K have been reported [7]. Here the spherical cap model becomes unrealistic, because the associated contact angle is so low as to make it impossible to construct a cap shape for the atoms in the critical nucleus. Other models have been proposed, notably the adsorption model of Kim and Cantor [8] in which the structure of a monolayer absorbed on a substrate can change sharply from liquid to solid as temperature is decreased. With either the spherical cap or the adsorption model, a nucleus can form on a particle surface of radius much less than the radius of curvature of the critical nucleus.

Once the particle surface is covered, Fig. 1(a), subsequent thickening of the solid Al, Fig. 1(b), reduces the radius of curvature of the growing solid until the hemispherical condition is reached, Fig. 1(c). Thereafter, growth results in an
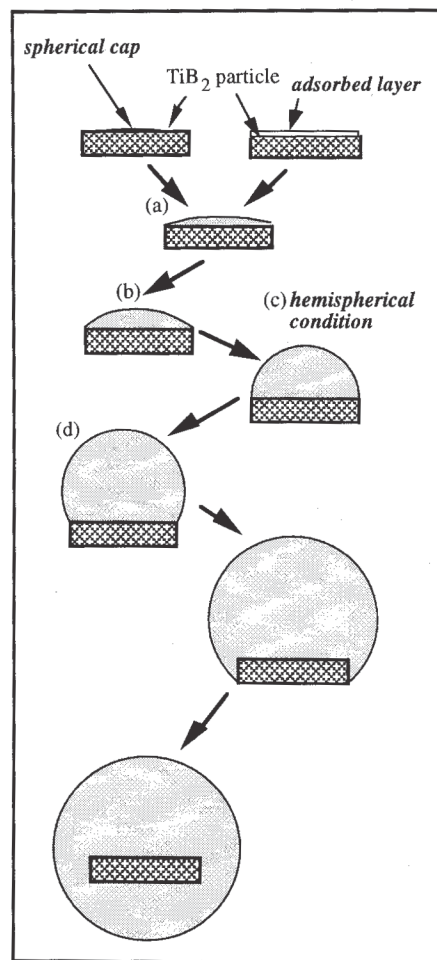

Fig. 1. Schematic diagram to show the growth of solid Al on the surface of the inoculant particle following nucleation or adsorption. For clarity, growth is shown only on the top (0001) basal face of the TiB_2 particle. In practice, growth is likely to occur on both top and bottom faces.

increase in the radius of curvature (Fig. 1(d)). The minimum radius of curvature of the solid/liquid interface, Fig. 1(c), corresponds to a maximum in equilibrium undercooling. Free growth occurs from the particle surface only if its basal face radius is greater than the critical growth radius at the relevant temperature, given by [9]:

$$r^* = \frac{2\sigma}{\Delta G_v} \qquad (1)$$

where σ is the interfacial energy between solid and liquid phases, and ΔG_v is the free energy decrease per unit volume of solid formed (taken to be $\Delta S_v \times \Delta T$ (see eq. (2)), where ΔS_v is the entropy per unit volume of aluminium and ΔT is the undercooling below the liquidus temperature). Hence the size of the particle required to support free growth decreases with increasing undercooling. During cooling the largest particles in the melt will become active growth centres first. It is proposed that for a particle to behave as an active growth centre, the barrier is that for free growth, not for the initial nucleation event. For free growth there are **no stochastic**

effects (as would be found for nucleation); a distribution of sizes translates directly to a distribution of initiation temperatures for growth. It is assumed that all particles have a very high nucleation potency for α-Al. The deterministic nature of free growth necessitates using a distribution of particle sizes in the modelling. As seen later (Fig. 6), a large range of particle size is evident.

<u>Calculation Procedure</u>

The model simulates the variation of temperature with time for a fixed volume of isothermal, molten, commercial purity aluminium (99.7 wt.%), containing refiner particles, under an imposed heat extraction rate. The calculation is performed over variable time increments; if the temperature change is increasing over successive time increments the next increment is reduced, and vice versa. The assumption, as in [5], of isothermal melt conditions is reasonable as the thermal diffusion length is 6 to 7 orders of magnitude greater than the nucleus separation.

The temperature of the melt is controlled only by the imposed heat extraction rate, until the undercooling is sufficient to allow free growth on the largest particles in the system, when latent heat release will also contribute, eventually causing the melt to become recalescent. Inoculants are exposed to a maximum undercooling (in this work ~0.3 K), defining the minimum particle size able to support growth. As solidification proceeds the release of latent heat causes re-melting, so the actual minimum active particle size is slightly larger than that corresponding to the point of recalescence (Fig. 2).
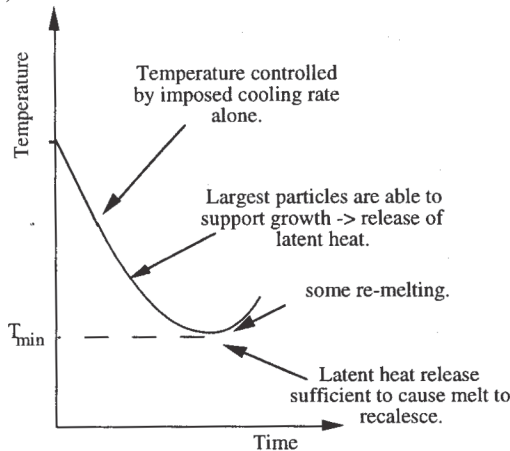

Fig. 2. Schematic diagram of variation of temperature with time for initial cooling sequence in the melt.

The melt contains many inoculant particles each having a characteristic growth temperature, T_{growth}, given by:

$$T_{growth} = T_{liq} - \left(\frac{2\sigma}{\Delta S_v r_p}\right) \quad (2)$$

where T_{liq} is the liquidus temperature and r_p is the particle radius. The variation of temperature with time is given by a simplified heat balance between thermal losses represented by an imposed cooling rate prior to solidification, R, and the latent heat emitted per unit volume of melt, Q, summed for the whole particle size distribution. The temperature of the melt in one time increment, $T_{(j)}$ is related to that in the previous increment $T_{(j-1)}$ by:

$$T_{(j)} = T_{(j-1)} - Rdt + \frac{Q}{C_v} \quad (3)$$

where C_v is the heat capacity per unit volume for liquid Al and dt the time over which the temperature change is calculated.

<u>Calculation of growth rate</u>

The radius of solid growing from the inoculants, r, varying with time, t, is given by an isothermal approximation [5]:

$$r = \lambda_s (D_s t)^{1/2} \quad (4)$$

Differentiating eq. (4) with respect to t, and substituting back gives the growth rate, V:

$$V = \frac{\lambda_s^2 D_s}{2r_{(j-1)}} \quad (5)$$

where $r_{(j-1)}$ is the radius of the growing solid in the previous time step, and D_s is the solute diffusion coefficient in the liquid. For the low solute level in this work, eq. (5) applies to a good approximation, even in the non-isothermal case, for successive time increments. The present work focuses on commercial purity aluminium (~99.7 wt.%), the major impurities are iron and silicon. This model considers only the effect of iron in solution, although it is acknowledged that other elements in solution, like Ti from the added refiner, may also contribute to the total solutal undercooling [6]. λ_s is given by [5]:

$$\lambda_s = \left(\frac{-S}{2\pi^{1/2}}\right) + \left(\frac{S^2}{4\pi} - S\right)^{1/2} \quad (6)$$

Assuming diffusion-controlled growth, S is given by:

$$S = \left(\frac{-2(\Delta T - \Delta T_c)/m}{(k-1)\left[C_A - (\Delta T - \Delta T_c)/m\right]}\right) \quad (7)$$

where:

$$\Delta T = m(C_A - C_{IL}) \quad (8)$$

and:

$$C_{IS} = kC_{IL} \quad (9)$$

where C_{IL} and C_{IS} are the liquid and solid interface concentrations respectively, C_A is the bulk liquid concentration, k is the (constant) distribution coefficient, m is the liquidus slope, ΔT is the melt undercooling below the liquidus temperature, and ΔT_c is the curvature undercooling associated with the growing solid, given by:

$$\Delta T_c = \frac{2\sigma}{\Delta S_v r} \quad (10)$$

Hence the growth rate is a function of the undercooling and radius of the growing crystal. Note that $T_{(j)}$ is calculated using $V_{(j-1)}$ for $r_{(j-2)}$ otherwise the growth of solid would never extend beyond the equilibrium hemispherical condition. In all calculations the values of C_A, k, and m were 0.3 wt.%, 0.02 and 2.78 K wt.%$^{-1}$ respectively.

Growth morphology The growth rate laws applied here assume spherical growth. This is verified by comparing computed radii with the radii for absolute and relative stability of spheres of solid [10], Fig. 3; all growth will be spherical until after the point of recalescence.
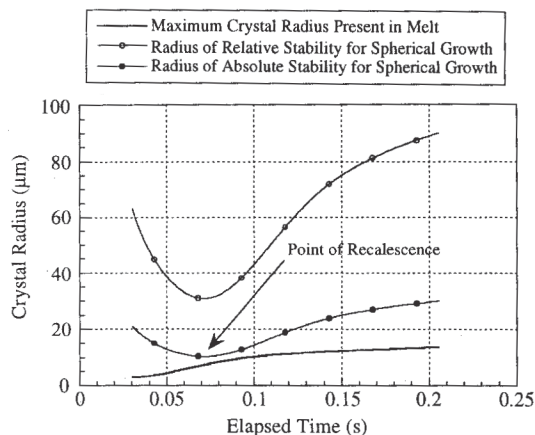

Fig. 3. The maximum crystal radius present in the melt for the 'good' (next section) refiner (cooling rate 2 K s^{-1}, addition rate of 1 kg tonne^{-1}) shown with calculated critical radii of relative and absolute stability for spherical growth.

Assuming no interference between particles, a final grain size can be calculated. This assumption is supported by the small solid fraction at recalescence, and is in agreement with [5] — the solute diffusion fields around crystals are usually much smaller than the interparticle separation.

Crystal re-melting If, after recalescence, any crystals reach the state where their current curvature undercooling is greater than the current bulk undercooling, they must dissolve; at this point their heat of melting is included in the overall heat balance. This effect was investigated by monitoring the active number of growth centres with time, Fig. 4. A small proportion of crystals re-melt after recalescence, but the effect on the final grain size is very low (~ 1 µm increase). The number of active particles after recalescence corresponds to ~0.75% of the total number of particles present in the melt.

Particle Size Distribution

The size distributions of particles in a 'good' and 'poor' Al-5Ti-1B wt.% refiner rod (courtesy of London and Scandinavian Metallurgical Co. Ltd.) were studied, using optical microscopy, scanning electron microscopy (SEM) and image analysis. Samples were mounted in conducting bakelite, polished, and etched using Poulton's reagent. The optical micrographs show macroscopic details, such as the degree of banding of particles along the rolling direction of the refiner rod, while the individual particle size distribution is obtained from SEM, Fig. 5.

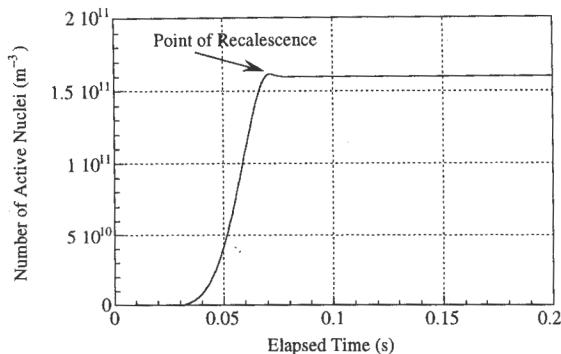To obtain the size distribution from the section of the sample

Fig. 4. The number of growth centres with time, for the good refiner (next section) with a cooling rate of 2 K s^{-1} and addition rate of 1 kg tonne^{-1}. The decrease after recalescence is due to re-melting of most recently activated growth centres; after this the number remains constant as no more activation is possible.
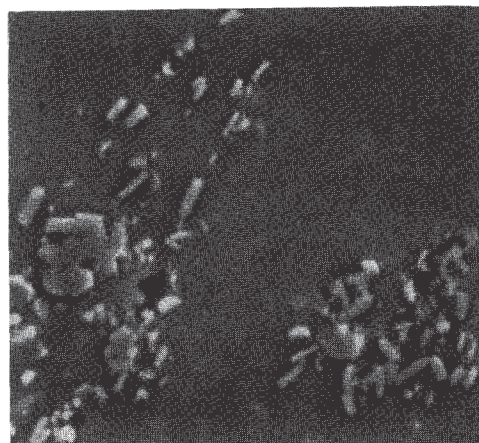
3 µm

Fig. 5. SEM picture showing microstructure of 'good' refiner; the light areas represent individual TiB$_2$ particles.

stereological corrections had to be applied. The raw data were assigned into bins and normalised to account for the observed areal density being proportional to the average particle radius in the bin. The shape of the computed true size distribution is shown, for the good refiner, in Fig. 6.

The populations at small particle sizes may have contributions from surface scratches on sample sections wrongly interpreted in the image analysis. The size distributions in the two refiners were very similar, ranging between 0.2 and 6 µm, best fitted by exponential curves of the form:

$$y = \exp\left(-\frac{d}{d_0}\right) \qquad (11)$$

where d is the particle diameter and d_0 is the characteristic width of the distribution. For the good and poor refiners the values of d_0 were 0.56 µm and 0.45 µm respectively. Thus, the poor refiner had a somewhat steeper distribution with fewer
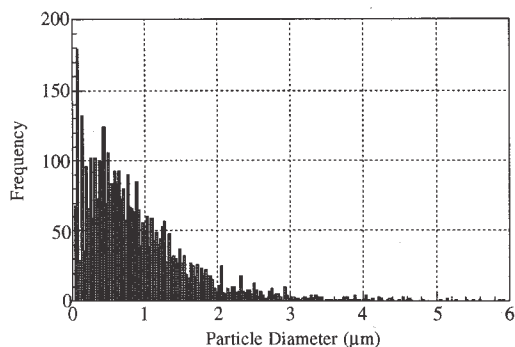
Fig. 6 Size distribution of TiB$_2$ particles in a 'good' Al-5Ti-1B refiner rod.

Fig. 8. Comparison of the predictions in the present work and in [5] of the number of grains as a function of the number of added particles. The work in [5] clearly shows two regimes, (a) and (b); the behaviour in (a) represents 100% efficiency.

size range was estimated assuming a constant total volume of TiB$_2$ for a fixed addition rate. There is still some uncertainty in the size distributions because of the approximation in calculating a 3D population from 2D measurements. While the particle size distribution between 0.2 μm and 6 μm is well modelled by an exponential curve, the sharp cut-off at each end must be unrealistic. Although in this instance the measured particle size distributions are very similar, the model could be a useful tool for predicting the behaviour of refiners whose particle size distributions vary greatly.

Grain Size Prediction

The model, taking the particle size distribution for the good refiner, was used to predict the influence of varying the addition rate of Al-5Ti-1B refiner on grain size, Fig. 7.
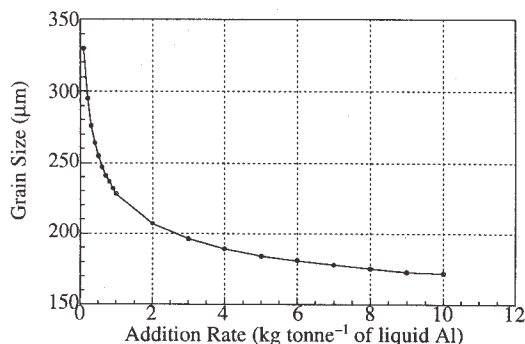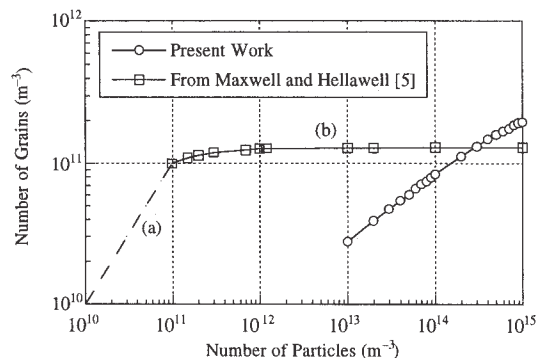

Fig. 7. Effect of addition rate on grain size for the good refiner under an imposed cooling rate of 2 K s^{-1}. It is shown that heavy addition of refiner does not give a noticeably finer grain size after a saturation level is reached.

In agreement with practice, as refiner is added to the melt the grain size decreases at first rapidly and then more slowly, representing an effective saturation. The decrease in efficiency at higher addition levels was found also by Maxwell and Hellawell [5], but as shown in Fig. 8, there are substantial differences in the predictions.

The sharp transition between (a) and (b) (Fig. 8) is not found in the present work, where efficiencies of 100% are not approached, despite the grain size range being similar to that in [5]. The key difference in the modelling is in the distribution of inoculant particle characteristics. In [5],

although the effects of differing nucleation potency (contact angle) were studied, all calculations were performed for populations of particles of uniform potency. The stochastic nature of the nucleation ensures that the nucleation occurs over a range of undercooling, but at any undercooling all inoculant particles would become active after sufficient time; in this way 100% efficiency can be approached. In contrast, in the present work the size distribution of particles restricts the fraction of them which can be centres for free growth at any undercooling. The exponential nature of the distribution (Fig. 6) means that a large fraction of the particles may never reach the undercooling at which they could become active.

The regime (a) in [5] (100% refining efficiency, Fig. 8) arises from the assumed uniform particle characteristics. Any distribution of characteristics leads to the impossibility (as discussed above) of obtaining 100% efficiency at all, and blurs the transition between more efficient and less efficient regimes (i.e., between low and high addition levels). This blurring is evident in the present work (Fig. 8) arising from the imposed distribution in particle size. It could equally arise however, if the heterogeneous nucleation model of Maxwell and Hellawell were adopted with a distribution in nucleation potency. Actual inoculant particles seem unlikely to be uniform in their characteristics, and the contrast in the predictions in Fig. 8 shows the importance of taking them into account in matching experiment and modelling.

The model, with input of the measured particle size distributions, was also used to compare the performance of the 'good' and 'poor' refiners with cooling rate, Fig. 9. The model predicts a variation of grain size with cooling rate in accord with experience, but it does not differentiate significantly between the behaviour of the poor and good refiner. In long-term TP1 [11] grain-refining tests the poor and good refiners give grain sizes of ~500 μm and ~120 μm respectively, but it seems from Fig. 9 that this difference is not attributable to the (relatively small) difference in their particle size distributions. Other origins may be differences in the spatial distribution of particles or in the intrinsic nucleation potency of the refining particles. This again emphasises the importance of including distributions of particle characteristics.

The volume fraction of solid at recalescence was ~10^{-4} (in agreement with [5]), and the errors incurred in the heat balance calculations were typically 0.04%.
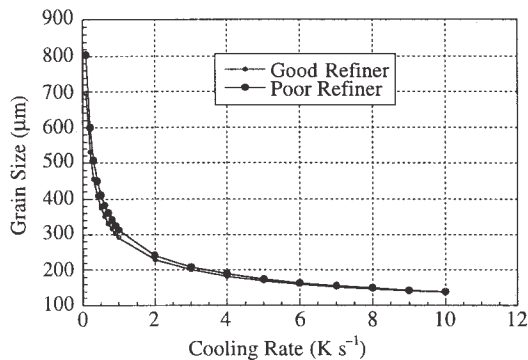
Fig. 9. Variation of grain size with cooling rate for the good and poor refiner, both added at a level of 1 kg tonne^{-1}. The differences in the particle size distributions in the two refiners cannot explain the widely differing grain-refining performance that they are known to exhibit in practice.

Conclusions

The model of Maxwell and Hellawell [5] highlights the importance of melt recalescence in limiting the grain-refining efficiency of inoculants added to aluminium. It has been shown in the present work that the barrier to free growth of α-Al from inoculant particles may be significant and may determine the undercooling at which growth becomes possible, rather than the heterogeneous nucleation potency considered in [5].

The Maxwell-Hellawell model has been adapted to the case in which the undercooling at which growth starts is strictly determined by inoculant particle size according to the free-growth criterion. In the modelling it is necessary to consider a distribution of particle size. The modelling includes the effects of remelting due to recalescence, though this is found to have a negligible effect on final grain size. The assumption in the Maxwell-Hellawell model of spherical growth is further examined, and is found to be justified in the regime of interest.

Size distributions of inoculant (TiB_2) particles have been determined in refined samples using SEM and image analysis. A broad range of diameter is found, from 0.2 μm to 6 μm. In the size range of interest, the populations decrease exponentially with increasing diameter. Similar size distributions were found in two refiners of significantly different performance ('good' and 'poor'), the size distribution in the 'good' refiner being somewhat more broad.

The Maxwell-Hellawell model adapted for free growth has been applied with a particle size distribution matching that measured for the 'good' refiner. Grain size can be predicted as a function of addition level. The refiner efficiency decreases as the addition level is increased, but there is no sharp transition in the efficiency as found by Maxwell and Hellawell in the original model. The transition is blurred by the distribution of inoculant characteristics.

The free-growth model predicts that a finer grain size is achieved at greater cooling rates, in agreement with experience. However, it does not predict any significant difference in performance of the 'good' and 'poor' refiners arising from their different particle size distributions. This suggests that the distributions of particle position and nucleation potency also have some influence.

The present modelling successfully predicts refiner efficiencies of the order of 1%. It is concluded that any distribution of characteristics of inoculant particles within a refiner will have a large effect on how the efficiency of the refiner varies with addition level. Quantitative testing of the modelling is still required.

References

1. P. Schumacher et al., "New studies of Nucleation Mechanisms in Al-Alloys: Implications for Grain-Refinement Practice," Mater. Sci. Technology, in press.

2. P. Schumacher and A. L. Greer, "High-Resolution Transmission Electron Microscopy of Grain-Refining Particles in Amorphous Aluminium Alloys" Proc. Conf. 'Light Metals 1996', ed. W. Hale (Warrendale, PA: TMS, 1996), 745-753.

3. D. G. McCartney, "Grain-Refining of Aluminium and its Alloys using Inoculants," Inter. Mater. Rev., 1989, **34**, 247-260.

4. O. M. Suarez and J. H. Perepezko, "Microstructural Observation of Active Nucleants in Al-Ti-B Master Alloys," Proc. Conf. 'Light Metals 1992, ed. E. R. Cutshall (Warrendale, PA: TMS, 1992), 851-859.

5. I. Maxwell and A. Hellawell, "A Simple Model for Grain Refinement During Solidification," Acta Metall., 1975, **23**, 229-237.

6. F. Hodaj and F. Durand, "Equiaxed grains in Multicomponent Alloys: Effect of Growth Rate," Acta Metall. Mater., 1997, **45**, 2121-2127.

7. L. Backerud and S. Yidong, "Grain-Refining Mechanisms in Aluminium as a Result of Additions of Titanium and Boron, Part 1," Aluminium, 1991, **67**, 780-785.

8. W. T. Kim and B. Cantor, "An Adsorption Model of the Heterogeneous Nucleation of Solidification," Acta Metall. Mater., 1994, **42**, 3115-3127.

9. W. Kurz and D. J. Fisher, Fundamentals of Solidification (Switzerland: Trans Tech Publications Ltd., edn.3, 1992), 22-26.

10. W. W. Mullins and R. F. Sekerka, "Morphological Stability of a Particle Growing by Difusion or Heat Flow," J. Appl. Phys., 1963, **34**, 323-329.

11. G. P. Jones and J. Pearson, "Factors Affecting Grain Refinement of Aluminium using Ti and B Additives," Metall. Trans B, 1976, **7**, 223-234.